THE PRE-X LIFTING BODY COMPUTATIONAL FLUID DYNAMICS AND WIND TUNNEL TEST CAMPAIGN

Authors

Paolo Baiocco*, Sylvain Guedron*, Jean Oswald*, Donatella Ponziani*,
Marc Dormieux†, Emmanuel Cosson†,
Jean-Pierre Tribot‡, Alain Bugeau‡

* CNES Direction des Lanceurs
Rond Point de l'Espace – 91023 Evry Cedex, France
Phone : +33 (0)1.60.87.72.14, Fax : +33 (0)1.60.87.72.66
E-mail : paolo.baiocco@cnes.fr, sylvain.guedron@cnes.fr,
Jean.oswald@cnes.fr, donatella ponziani@cnes.fr

† ASTRIUM SAS
Avenue du Général Niox – BP1, 33165 Saint-Médard-en-Jalles Cedex, France
Phone : +33 (0)5.56.57.20.70, Fax : +33 (0)5.56.57.32.84
E-mail : marc.dormieux@astrium.eads.net; emmanuel.cosson@astrium.eads.net

‡ Dassault Aviation
78, Quai Marcel Dassault – Cedex 300 92552 St Cloud Cedex, France
Phone : +33 (0)1.47.11.37.60, Fax : +33 (0)1.47.11.57.95
E-mail : jean-pierre.tribot@dassault-aviation.fr; alain.Bugeau@dassault-aviation.fr

ABSTRACT

Pre-X is the CNES proposal for demonstrating the maturity of European technology for gliding re-entry spacecraft. The main goal of this experience is to demonstrate the implementation of reusable thermal protections, perform aero thermo dynamics experiments and efficiency of a suitable guidance navigation and control system. The attitude control is realised by elevons and reaction thrusters overall the hypersonic flight, with a functional and experimental objective.

The Pre-X program is achieving the Preliminary Design Revue during year 2007. In the preceding phases, the aerodynamic shape and centring have been consolidated. The Pre-X project has been conducted up to now with the aim of joining the IXV program.

During phases A and B a number of wind tunnel tests has been performed for the vehicle aerodynamic and aerothermal characterisation, together with computational fluid dynamics. These tests permitted to cover the Mach range from 0.8 to 14 and to investigate the main effects of aerodynamic and aerothermal phenomena.

The logic and main results of this activity are presented in this paper.

INTRODUCTION

The current Pre-X baseline mission is performed by the VEGA launch vehicle in a quasi equatorial ballistic trajectory. The spacecraft makes an almost complete earth revolution before splashing down on the Pacific Ocean. The vehicle re-entry point is at 120 km and the mission objectives are fulfilled between Mach 25 and 5. Then the vehicle has to pass to subsonic speeds (either under drog chute or by controlled symmetric flight), the main chute opens and it is finally recovered in the sea. Nominal flight foresees an impact at the mean way between Galapagos and Marquise islands. There the spacecraft is recovered by boat.

The hypersonic supersonic aerodynamic data base has been assessed via Euler and Navier-Stokes modelling. Euler data have been used to refine the aerodynamic data base in terms of Mach number, angle of attack, flap setting, while Navier-Stokes to consolidate the viscous effect implemented in the data base by previous phases.

The aerodynamic tests have been performed in the TsAGI wind tunnels T-128, T-116 and T-117, the ONERA wind tunnel F4, the VKI longshot. The Mach range covered by these tests and CFD is from M=0.8 to M=25.

The ATD tests in the TSNIIMASH facility PGU7, the DLR HEG and the ONERA R2Ch. The Computation

Fluid Dynamics (CFD) has been used to rebuilt these tests and compare numerical with experimental solutions. The equivalent actual flight conditions have also been simulated.

The ATD characterisation has been used in order to size the thermal protections and find the most suitable architecture.

PRE-X REQUIREMENTS

This project addresses a first generation of re-entry experimental vehicle necessary in Europe for risk mitigation before opening the way for future spacecraft applications. Due to atmospheric re-entry specificity in terms of environment and phenomena, ground based experiments are not always representatives and in flight experimentation is mandatory. In-flight experimentation which cannot be simulated on ground will be performed by means of Pre-X. The flight control by means of body flaps is the first time to fly in Europe, as well as a complete fully reusable TPS architecture. A procurement specification has been assessed for the Pre-X vehicle including the following constraints:

- Mission objectives are covered between Mach 25 and Mach 5.
- No active oxidation during nominal trajectory .
- Recovery of vehicle and measures is mandatory.
- TPS expertise and dismantling without damage is mandatory.
- Recovery in sea and buoyancy greater than 48h.
- Possibility to fly both on the VEGA and DNEPR launch vehicles, with VEGA as baseline.
- Mission reliability 0.95 after separation of launcher.
- Safety criteria lower than 10^{-7} to do a victim.
- Ambitious design to cost objective, excluding launch.
- Year of flight: 2010.

VEHICLE GEOMETRY AND MASS BUDGET

The vehicle shape is depicted in Fig.1. The mass and centre of mass positions are given in Tables 1 and 2. Three items are defined: nominal, with margins and a maximum value. The vehicle is about 5 m long (including elevons) and 2 m wide.

Table 1 – Pre-X mass (kg)

Minimal	Maximal
1440	1900

Table 2 – Centre of mass coordinates (mm)

x back	y	z up
1484	0	-120

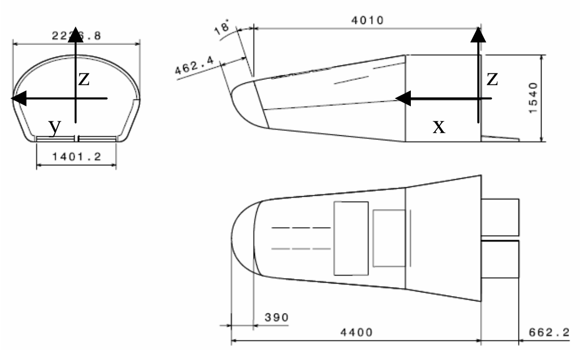

Fig. 1 – Pre-X geometry

LOGIC AND TEST PLAN

From the vehicle requirement it is apparent that the main domain of investigation concerning aerodynamics and ATD is the hypersonic range. The vehicle has been designed in order to have get good flying qualities and ATD similarity with full scale spacecraft from Mach 25 to 5. However, the vehicle performance for Mach numbers below 5 is important to take the vehicle in safe conditions up to parachute opening.

The transonic region can be passed in two ways:

- **Supersonic scenario**: A drogue chute opens at about Mach 1.5, then the main parachute is opened ones, reached suitable conditions.
- **Subsonic scenario**: A main chute opens at a descent velocity of about 65 m/s and takes the vehicle to a descent velocity of about 9 m/s.

For this reason tests and computations on fluid dynamic codes have been performed up to Mach 0.8 and an Aero Dynamic Data Base (AEDB) computed for the Mach range from 25 to 0.8.

The test campaign for aerodynamic and ATD characterisation has been assessed on the base of the nominal Pre-X re-entry trajectory and main phenomena to be investigated.

The main similarity parameters considered are:

- $Re = \frac{\rho V L}{\mu}$ for viscous effects on elevons and nose
- ρL (dissociation parameter) for real gas effects
- q for thermal flux at stagnation point
- Mach number.

The wind tunnel test campaign for aerodynamics and ATD has been performed in the facilities listed in Tables 3 and 4.

These facilities performances are placed on the Reynolds versus Mach number re-entry trajectory profile in order to assess the aerodynamic similarity with respect to Pre-X flight conditions (Fig. 2).

The similarity law for ATD is given in Fig. 3 and Fig. 4 respectively for the dissociation parameter ρL and nose heat flux.

Table 3 – Aerodynamic facilities

Regime	Facility	Company
Transonic-Sup.	T-128	TsAGI
Supersonic	T-116	TsAGI
Hypersonic	T-117	TsAGI
Hypersonic	Long shot	VKI
High enthalpy	F4	ONERA

Table 4 – ATD facilities

Regime	Facility	Company
Hypersonic	R2Ch	ONERA
High enthalpy	HEG	DLR
Hypersonic	PGU-7	TSIIMASH

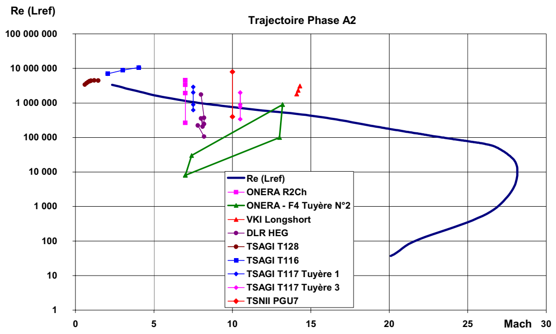

Fig. 2 – Re versus Mach along Pre-X trajectory

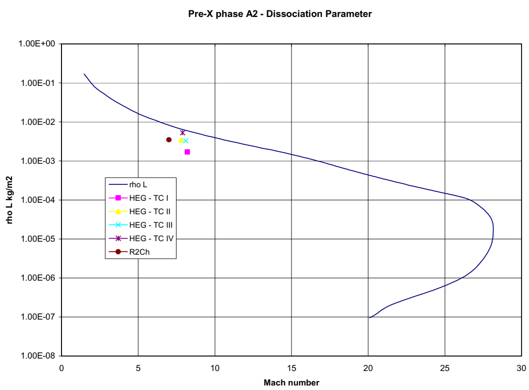

Fig. 3 – ρL versus Mach along Pre-X trajectory

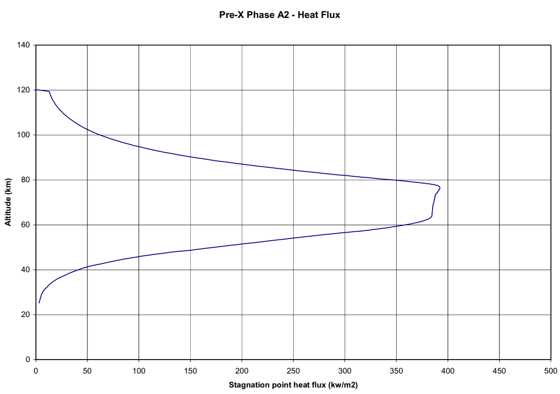

Fig. 4 – Nose heat flux along Pre-X trajectory

As it is well known, the above cited similarities cannot be realised all in once or even never. For example the ground facilities of Table 3 cannot realise Mach numbers greater than 14. For this reason most of the flight conditions above Mach 10 have been studied only with CFD.

Air chemistry plays an important role above Mach 5, producing the O_2 and N_2 dissociations, which depend on the Mach number itself. In particular, the shape and position of the shock wave is affected by this phenomenon and consequently the aerodynamic characteristics. In particular, the pressure distribution over the body surface, and hence the centre of pressure, change.

The effects of altitude plays a role on the velocity of chemical reactions occurring behind the shock: these reactions are faster at high static pressure. Hence at low altitudes there is more probability to get equilibrium conditions for dissociated molecules, while at high altitudes the non equilibrium condition is easier.

At high altitudes the Reynolds number is lower and viscous effects are more important giving rise to phenomena such as elevons control efficiency reduction and increased skin friction.

All the above cited phenomena have an impact on both aerodynamics and ATD and are one of the main concern of Pre-X flight experience. The other is the TPS material and architecture characterisation during the mission.

AERODYNAMICS

Mach numbers 10 and 25 have been chosen for performing intensive CFD characterisation, because of the lack of data from wind tunnels and most important air chemistry and viscous effects occurring in this flight regime.

For Mach number between Mach 4 and 10, the hypothesis of perfect gas for air with γ=1.4 has been considered, based on X-38 experience, where real gas effects are negligible in this range.

For Mach above 10, air in chemical equilibrium or in chemical non-equilibrium have been assumed.

For boundary layer regimes, the following hypotheses have been considered:

- $4 \leq M \leq 10$ turbulent boundary layer from the nose and downstream.
- M=17.75 laminar regime or sudden transition at elevons hinge line.
- M=25 laminar boundary layer for all computations.

Euler computations have been performed in the following flight conditions:

- Mach = 4, 7, 10, 14, 17.75, 25
- Angle of attack α=35°, 40°, 45°, 50°, 55°
- Sideslip angle β=0°, 5°
- Elevons deflection δ_e=-10°, -5°, 0°, 5°, 10°, 15°, 20°
- Ailerons efficiency δ_a=0°, 5°

The nominal Pre-X flight conditions are α=45°, β=0° overall the hypersonic phase.

Conventions about vehicle axes are given in Fig. 5. Other reference parameters are given below:

- Moments are computed with respect to the point centre of mass.
- δ_e=(right elevon deflection + left elevon deflection) / 2, δ_E=>0 for pitch down.
- δ_A =(right elevon deflection - left elevon deflection) / 2, δ_A >0 for right wing upward.

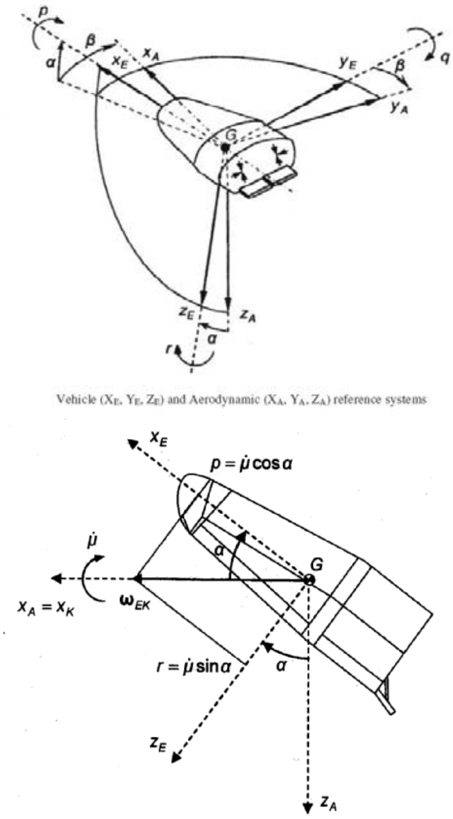

Fig. 5 – Pre-X vehicle and aerodynamic axes definition

WIND TUNNEL TESTS

This section gives the description of wind tunnel tests performed during the Phase A2/B of the Pre-X programme for the constitution of the aerodynamic data base (Table 3). The model used for all the TsAGI wind tunnel is the same and has a scale of 1/13.75. The sting is different.

T-128

The transonic-supersonic tests have been performed in the TsAGI wind tunnel test T-128 for angle of attack range 30÷85 degrees, Mach 0.8÷4, flap-ailerons deflection -10÷10 degrees. The sting effect has been assessed by means of 3D Navier-Stokes computations, as shown in Fig. 6. Fig. 7 shows the Pre-X model in the test section.

The result is that the longitudinal stability is assured for the angle of attack range 60÷90 degrees. The lateral stability needs to be consolidated with respect to ailerons efficiency even if it has been refined by these tests. In particular, the coefficient $C_{n\beta}$, defining the yaw moment (n) due to sideslip (β), is always positive and increases for decreasing Mach number.

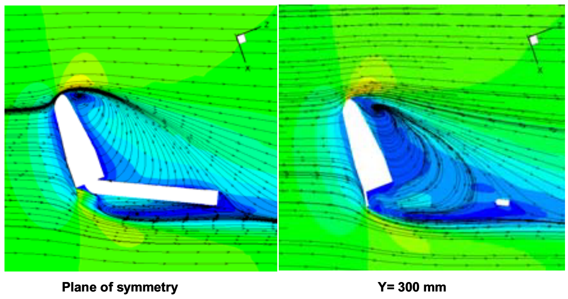

Fig. 6 – Pre-X sting effect for T-128

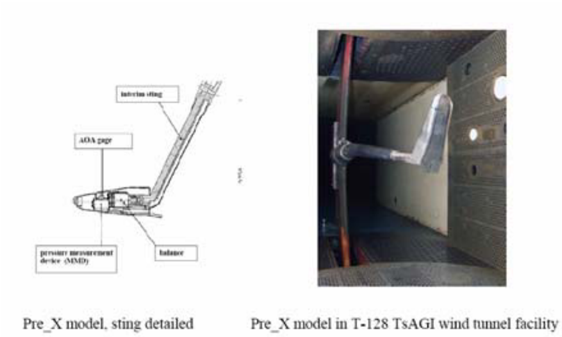

Fig. 7 – Pre-X in the T-128 transonic wind tunnel

T-116

In the supersonic regime, tests have been performed at Mach 2 and 4 in T-116. The Reynolds number is higher in the wind tunnel than during flight. This effect has been estimated by means of CFD and it is small with respect to elevons efficiency. However, at Mach 2 the Reynolds number effect is really negligible and the flow remains attached in the flap area (at least at flap deflection δ_E=10°). At Mach 4 a separation zone appears and it is slightly larger for the flight conditions (resulting from CFD analysis). The streamlines resulting from CFD are given in Fig. 8 at Mach 4 and Re 11 10^6. The report of results is not yet available.

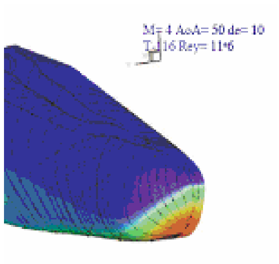

Fig. 8 – Pre-X streamline at Mach 4 in the T-116

T-117

The scope of T-117 tests is to validate the CFD computations in hypersonic flight and verify the lateral behaviour of the vehicle. The test campaign has been performed at Mach 7.5 and 10.5. The model scale is 1/13.5. The angle of attack range is 30°÷60°, the sideslip -10°÷10° and the flap deflection -10°÷15°. The nominal test conditions are summarised in Table 5.

An interesting result of this campaign is that C_m exhibits a non linear behaviour versus angle of attack due to shock structure modification, as shown in Fig. 9. This phenomenon is emphasized at δ_E=15°.

Mach	Re (10^6 m^{-1})	Re_{Lref}	p_0 (10^5 Pa)	T_0 (K)
7.5	3.22	1030000	12	712
70.5	2.	704000	43	1100

Table 5 – T-117 nominal test conditions

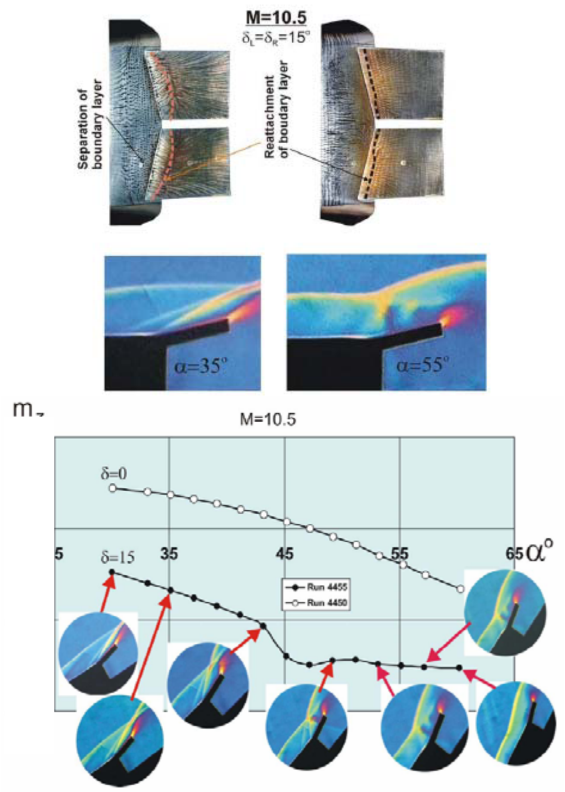

Fig. 9 – T-117: Flow patterns over the windward side

Long Shot

The VKI wind tunnel tests have been used to identify the hypersonic aerodynamics in longitudinal, lateral directions and the flap/ailerons efficiency. The M= 14 (contour nozzle) has been selected and nitrogen gas has been used, behaving as a perfect gas at such conditions. The scale of the model is 1/22 (Fig. 10). Since the standard aerodynamic balance is used, the accuracy of wind tunnel measurement for lateral aerodynamic components is less than for the longitudinal ones. A quite good agreement has resulted between CFD and WTT. Fig. 11 shows the comparison of the pitching moment versus flap deflections for different angles of attack.

Fig. 10 – Long shot 1/22 mock-up

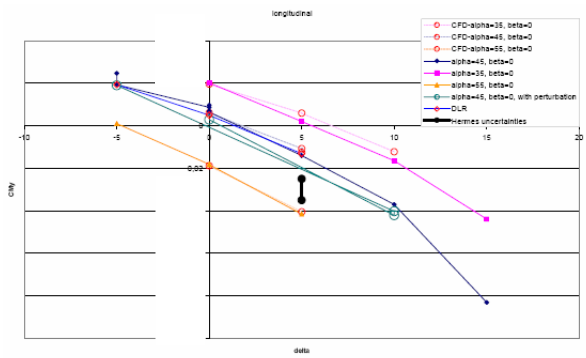

Fig. 11 – Pitching moment versus flap deflection for different angles of attack

F4

The aim of F4 test campaign was to determine the real gas effects on the aerodynamic forces and moments at the re-entry velocities and to compare the results with numerical predictions. Four flap deflections have been investigated, namely 0°, 5°, 10°, 15° with angle of attack 45° and 0° sideslip. The specified test conditions were: total enthalpy of 12 MJ at stagnation pressure of 300±10 bar in air. The model scale is 1/12.5 (Fig. 12). For different reasons the specified test conditions have not been reached. Instead the following values have been obtained:

- Total pressure p_0: 280 bar

- Total enthalpy h_0: 14.5 MJ/kg

An enthalpy effect on global aerodynamic coefficient has been pointed out, but an actual real gas effect during this campaign cannot be assessed before further analysis.

The CFD prediction of the F4 has been performed by means of Euler computations assuming thermo-chemical non equilibrium flow field for two kind of F4 conditions, summarised in Table 6.

The real gas seems poor in the stagnation region, meanwhile it remains more significant on the flap itself (Fig. 13). As far as pitching moment evolution is concerned, the real gas effect induces a very smooth pitch down without flap setting. However for flap deflection of 10°, the pitch down is more significant and is equivalent to 2.5° flap setting (Fig.14). Due to real gas effect the bow shock is closer to the vehicle windward than for M=10 solution in perfect gas (Fig. 15, comparison of F4 and T-117 M=10 cold gas).

Fig. 12 – F4 test campaign: model set up

Enthalpy	ρ (kg/m^3)	V (m/s)	T_0 (K)
12	0.00068	4752	742.857
14	0.000536	5170.7	1071.428

Table 6 – F4 conditions used for CFD

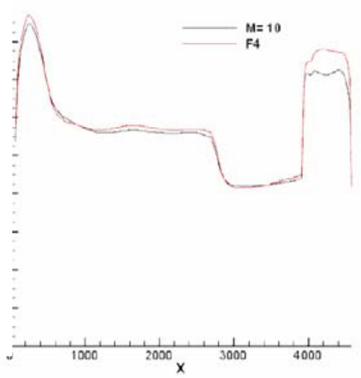

Fig. 13 – F4 CFD results: pressure coefficient on lower surface at section y=300 mm, AoA=45°, de=10°

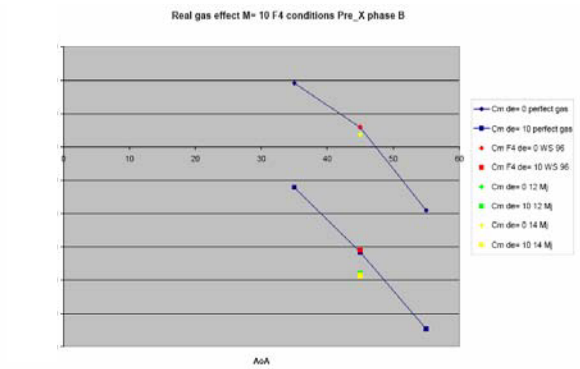

Fig. 14 – Real gas effect prediction on c_m

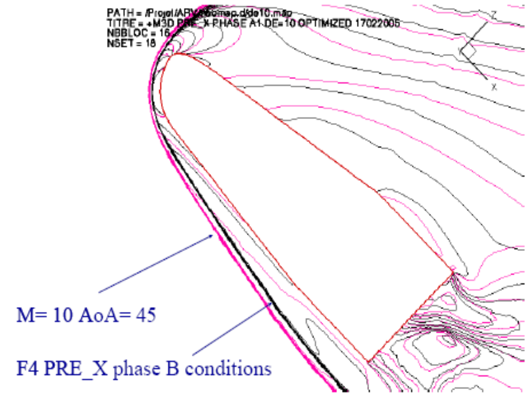

Fig. 15 – CFD comparison between perfect gas and F4 conditions

CONCLUSION ON AERODYNAMICS

The core of the AEDB is constituted by Euler computations. The discrepancies on the results among codes are well below the aerodynamic uncertainties, namely one order of magnitude on global coefficients.

The viscous effects are assessed by means of Navier-Stokes computations at high altitudes for Mach numbers greater than 10 (DLR and ONERA). The effect of air dissociations impacts essentially the bow shock (generating a higher drag force), the elevons efficiency, the centre of pressure position.

The viscous effects on C_L and C_D are of the same order of magnitude than the AEBD uncertainty. These effects become significant on C_m for elevons deflections greater than 10°. The effect is increasing for increasing δ_E. It is important for M=25 and tends to vanish for M=17.75. A correlation to non equilibrium chemistry exists for M≥17.75.

A difference in terms of pressure distribution appears on the elevons for deflections greater than 10° between the equilibrium and non equilibrium solution. The effect of chemistry modelling on pressure distribution is depicted in Fig. 16. This translates into a change on pitching moment consistent at δ_E=20°.

The global longitudinal aerodynamic coefficients versus Mach number are given in Fig. 17 for α=45°. Values for Mach number greater than 10 are taken from real gas at non equilibrium solution in laminar conditions. The aerodynamic efficiency changes slightly in the Mach range 4 to 25. The pitching moment is a negative derivative function versus angle of attack and is null for about α= 47° for zero elevon deflection and Mach=10.5. Fig. 18 shows this case in comparison with the T-117 results in these conditions. The difference between CFD and WTT is always low, but becomes greater for higher α.

Real gas effects are effective up to Mach 10, mainly on drag coefficient, placing the real value above the upper boundary of the uncertainty, whatever the elevon deflection (Fig. 19).

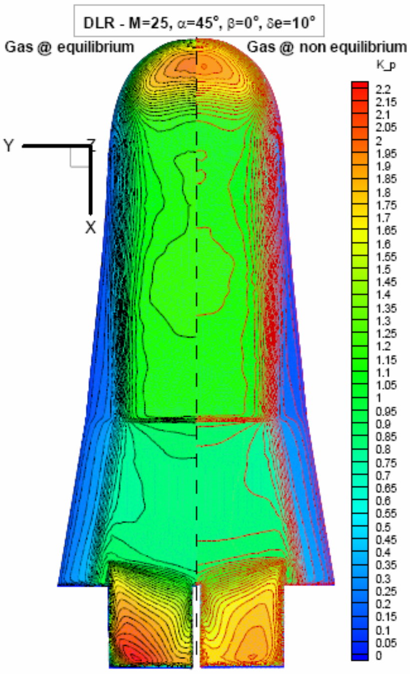

Fig. 16 – Effect of chemistry modelling on c_p

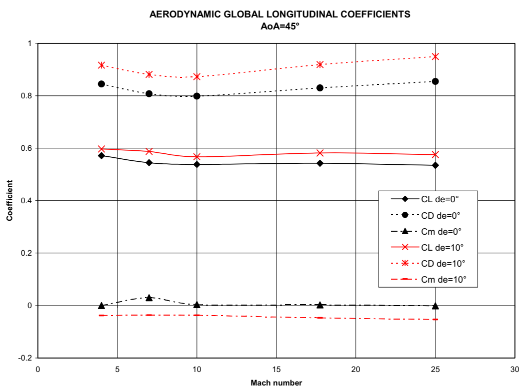

Fig. 17 – Global longitudinal aerodynamic coefficients

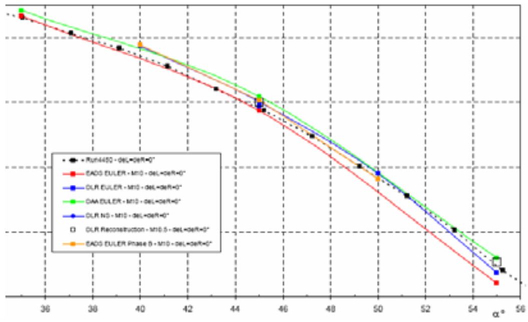

Fig. 18 – Pitching moment coefficient, M=10°, δ_E=0°

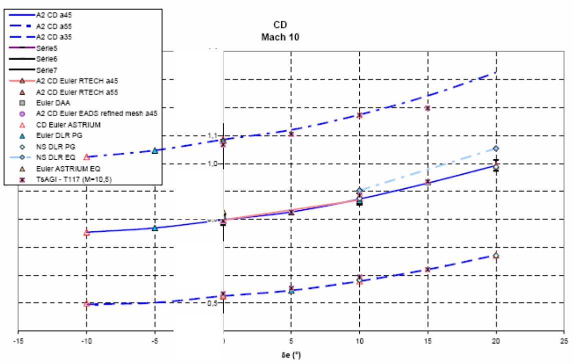

Fig. 19 – Drag coefficient, M=10°, δ_E=0°

Derivatives of aerodynamic coefficients, such as $\partial C_y/\partial\beta$, $\partial C_l/\partial\beta$, $\partial C_n/\partial\beta$, with respect to sideslip and weakly dependent on elevon deflections. This results from CFD and is confirmed by the T-117 results. The introduction of viscous effects and air chemistry at Mach 25 induces signification variations on side force and yawing moment coefficient derivatives. A good agreement on lateral coefficients between CFD and T-117 is obtained.

FLYING QUALITIES

The main goal of the flying qualities consists in:

- Guarantee the longitudinal and lateral stability and controllability.
- Estimate the maximum sideslip and elevon deflection needed for longitudinal and lateral trim.

The flight qualities have been computed with a given uncertainty on the Pre-X MCI.

Stability

- Longitudinal dynamic short period mode is always statically stable with worst case off nominal static margin greater than 4.5%.
- Lateral Dutch roll dynamic oscillation remains stable within the required margin ($C^*_{n\beta}>10^{-3}$).

Longitudinal and lateral trim

- Maximum longitudinal deflection needs remain in the range of about ±7°.
- The Lateral Control Departure Parameter (LCDP†) remains always negative insuring lateral/directional stability.
- Worst off nominal sideslip needs are $\beta<5°$ for Mach<2 and <6° for Mach>20.
- Worst off nominal asymmetric deflection are $\delta_A<17°$ for Mach=2 and $\delta_A<10°$ for Mach>8.

Almost all the available elevon deflection is used for longitudinal trim at Mach>10. This value is greater that the maximum allowable 8° due to thermal constraint. In addition, lateral trim must be achieved at the same time. These results have been obtained with the MCI uncertainties.

Moving the centre of mass forward helps reducing the longitudinal trim deflection need and is also favourable for lateral/directional flight qualities. The vertical position must be kept. In this case the deflection envelope is decreased. However, also in this case the maximum deflection constraint of $\delta=8°$ is not fulfilled. A possibility to reach lateral trim satisfying the maximum allowable elevon deflection, consists in using a movable mass along the y axis together with sideslip and a centre of mass at x_{cm}=58%. But in this case three control means are used: elevons, RCS, movable mass.

The proposed solution for vehicle trim must be confirmed by further analysis, including transients, control logic, feasibility of RCS control, updated AEDB.

The global deflection need for the two possible centre of mass positions is given in Fig. 20.

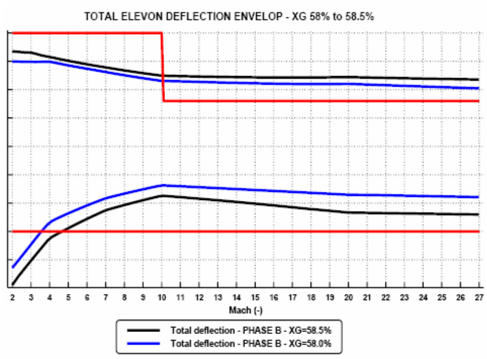

Fig. 20 – Global deflection needs

AEROTHERMICS

The objective the Aero Thermo Dynamic data Base (ATDB) is to provide heat fluxes for a selected control points on the vehicle along the flight path to provide input data for TPS sizing (Fig. 21). With this objective, investigations have been performed in phase A/B to characterise the Pre-X aero thermal environment during re-entry.

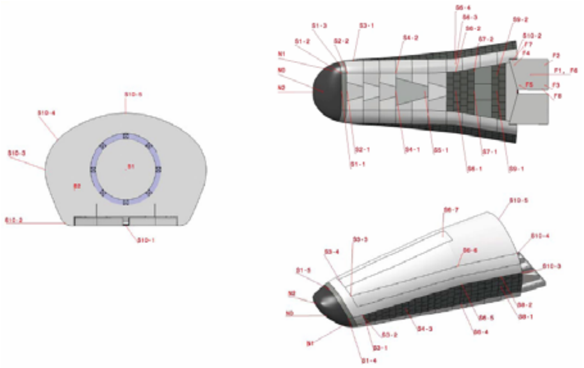

Fig. 21 – ATDB control points

CFD Euler plus boundary layer, Navier-Stokes computations and wind tunnel test in ONERA R2Ch, DLR HEG and TSIIMASH PGU7 have been performed. These tests give a contribution to investigation of laminar, turbulent and natural transition flow to give a contribution to the ATDB. An ATD plasma activity has been carried out in order to assess the radio frequency attenuation and black-out duration. In Pre-X black-out occurs between 105 and 47 km in the worst case.

The atmospheric density of the reference and sizing trajectories has been assumed together with an angle of attack of 35, 45, 55 degrees. Mach 7 and 10 computations were made with perfect gas assumption (γ=1.4), while Mach 17.75 and 25 were made with air at equilibrium. Other computations have been performed to consider the sideslip and laminar or turbulent regime. The wall was assumed to be in radiating equilibrium with a surface emission coefficient ε=0.8.

Fig. 22 shows the temperature map resulting from a Navier-Stokes computations in laminar conditions at Mach 25 and angle of attack 45 degrees. For turbulent computations the Wilcox k-ω method has been considered to better fit the R2Ch results than the Spalard Almaras and had been used as default.

---

† The LCDP is the vector product $\vec{u}_\beta \times \vec{u}_{\delta_A}$, where $\vec{u}_\beta = \left[C_{n\beta}, C_{l\beta}\right]^T, \vec{u}_{\delta_A} = \left[C_{n\delta_A}, C_{l\delta_A}\right]^T$. When the two vectors are collinear, the lateral/directional trim is impossible. The greater the Euclidean norm, the greater the trim capability is.

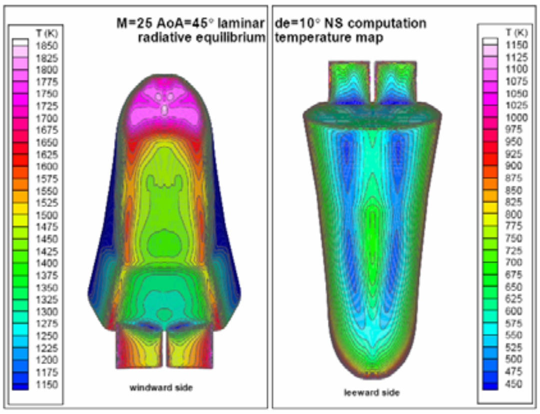

Fig. 22 - Laminar flow simulation: Navier Stokes CFD temperature for Mach 25, AoA=45°, de=10°

R2Ch

The model scale of R2Ch is 1/27.5 and the main goal of this campaign was to determine laminar to turbulent transition and SWBLI. The tests in the ONERA R2Ch and HEG wind tunnels have provided important information on vehicle general heating, laminar to turbulent transition, SWSWI, SWBLI and real gas effects.

Fig. 23 (left) shows a comparison between CFD computation and R2Ch results at Mach 7 in terms of heat flux. Fig. 23 (right) shows the shock visualisation. R2Ch is representative of Pre-X flight at Mach 7 and Reynolds number $1.4 \div 14 \cdot 10^6$ (Fig. 23). In particular, R2Ch runs have demonstrated a transitional interaction at Mach 7, AoA=35÷45 degrees for flaps deflections 15÷20 degrees. Viscous effects and laminar to turbulent transition have been investigated for different sideslips, Reynolds number, AoA, flap deflections. The extension of boundary layer separation decreases for increasing Reynolds. Some critical heating may exist on the body flap if a conservative margin policy is applied. The effect of the angle of attack with respect to shock waves interaction is shown in Fig. 24.

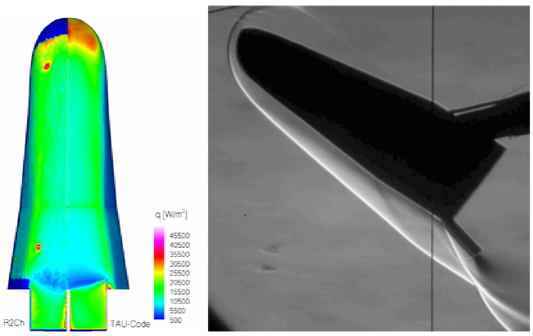

Fig. 23 - Laminar flow Navier Stokes CFD versus R2Ch (M=7) heat flux

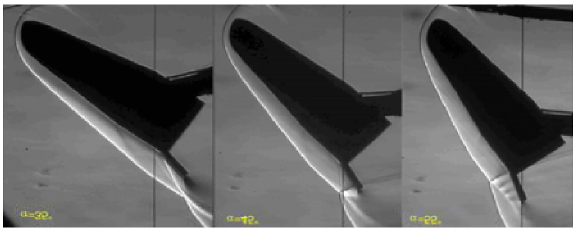

Fig. 24 – Effect of angle of attack at R2Ch (M=7)

HEG

The HEG test conditions are given in Table 9. The model scale is 1/13.75 and the stagnation enthalpy between 15 and 22 MJ/kg. Fig. 25 gives a comparison between computation and results from HEG at Mach 8 in laminar conditions at 45 degrees of angle of attack and flap deflection at 10 degrees. A comparison of the normalised pressure by means of CFD performed at DLR and HEG measurements shows a good agreement (Fig. 26). The main objectives of the campaign were the effect of angle of attack variation, the ailerons and sideslip effects, the elevon deflection effect on SWBLI.

h_0 (MJ/kg)	Mach	Re (10^5/m)	ρ (10^{-3} kg/m^3)
22	8.2	2	1.7
23	7.8	4.2	3.5
12	8.1	3.9	3.3
15	7.9	6.7	5.3

Table 9 – HEG test conditions

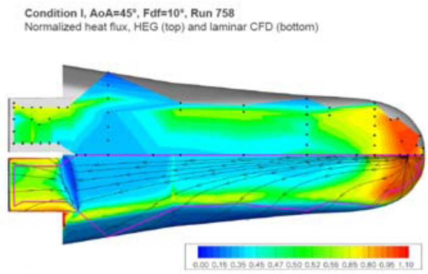

Fig. 25 – Heat flux: comparison CFD, HEG results at Mach 8, AoA 45° flap deflection 10°, laminar flow

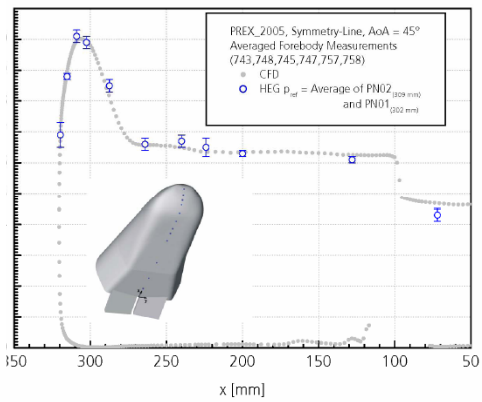

Fig. 26 – Normalised pressure from DLR HEG - CFD

PGU7

The main goal of the tests at PGU7 (TSNIIMASH) are to cross check the CFD and contribute to the final ATDB. The ranges of Table 10 have been investigated. Ten discrete heat flux measurements have been performed by using thermocouples in order to correlate the Infra-Red thermography on the windward and flaps. The use of a "medium" Reynolds number was supposed to reproduce a transitional SWBLI on the flaps (Re~3÷5 10^6). The test model at 1/15 scale is depicted in Fig. 27.

AoA (degrees)	40÷50
Sideslip (degrees)	0÷5
Flap deflection (degrees)	0÷15
Reynolds number	10^6÷6 10^6
Mach	~10.5
Effective test time (ms)	130

Table 10 – PGU7 test conditions

Fig. 27 – Model for PGU7 tests, scale 1/15

STEPS AND GAPS ASSESSMENT

A classical Space shuttle Reynolds type correlation is used to forecast laminar to turbulent transition along the trajectory for given protuberances due to TPS steps and gaps. A deeper analysis is ongoing in order to state the requirement in terms of maximum step and gaps compatible with maximum allowable heat fluxes, turbulence transition and vehicle assembly.

CONCLUSIONS ON AEROTHERMICS

The CFD and high enthalpy wind tunnel tests permitted to determine the heat flux and temperature evolution on the control points during re-entry, as well as the associated uncertainties. In particular, the core of the ATDB is constituted by the Euler plus boundary layer computations. Navier-Stokes and WTT are used for validation and uncertainty assessment.

The heat flux history for the worst case is shown in Fig. 28 for some control points referenced in Fig. 21. N0 is the stagnation point and F1 is the central point in the elevon. These results apply for a maximum flap deflection of 8°, constrained by the control law in order not to exceed the maximum C/SiC allowable temperature. In some specific points the temperature can slightly exceed the material allowable maximum temperature, but the time for which this occurs is usually short. In addition, this happens only in the most conservative case with phase B margins, to be reduced and refined in the successive phases.

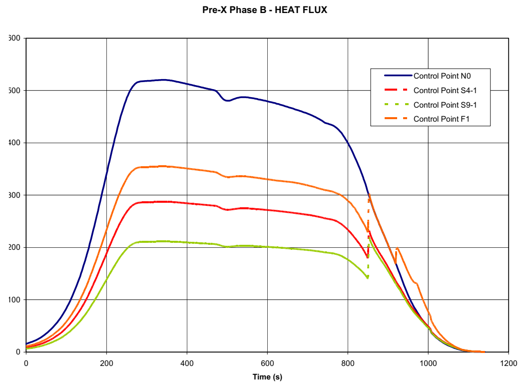

Fig. 28 – Heat flux versus time

SUMMARY AND CONCLUSION

Pre-X is the re-entry experimental hypersonic glider that CNES proposes as candidate for the IXV of the FLPP program. This is the necessary step for risk mitigation of future re-entry space planes or lifting bodies. The main goal of Pre-X is to demonstrate that Europe has the technology to master gliding re-entry of a reusable vehicle controlled by movable surfaces and jets.

For aerodynamic and ATD data base, wind tunnels tests have been performed in France, Germany, Belgium, Russia. A first assessment of the AEDB is based on CFD and WTT. In particular, most of the data are coming from Euler – boundary layer computations. Navier Stokes and wind tunnel tests have been used for a finer assessment of specific flight points and uncertainty evaluation.

The results of the ATDB have been used to size the TPS of the vehicle, on the base of the heat flux computed on specific control points. The flap heating is an important system constraint and the maximum flap deflection has been reduced in order to respect the maximum C/SiC allowable temperature.

The flying qualities have also been studied in detail and are satisfying at least in 2 to 25 Mach range, even if lateral control is sensible because of the Pre-X vehicle configuration. Below M= 2, preliminary flight qualities analysis demonstrated promising scenario enabling to fly properly in supersonic-transonic regime.

SYMBOLS

α	: angle of attack
β	: sideslip
ε	: thermal emissivity
μ	: bank angle
μ_i	: bank angle
ρ	: gas density
δ_A	: (right flap deflection+left flap deflection)/2
δ_E	: (right flap deflection-left flap deflection)/2
Θ	: flight path angle
c	: constant
cm	: centre of mass
C_L	: Lift coefficient
C_D	: Drag coefficient
C_m	: moment coefficient
$C_{n\beta}$,	: yaw moment (n) due to sideslip (β),
I_k	: inertia about *k* axis
L	: vehicle reference length (4.4 m)
M	: Mach number
Re	: Reynolds number
R_N	: nose radius
T	: gas temperature
V	: vehicle velocity
x_g	: x coordinate of vehicle centre of mass
y_g	: y coordinate of vehicle centre of mass
z_g	: z coordinate of vehicle centre of mass

GLOSSARY

AEDB	AErodynamic Data Base
ATD	Aero Termo Dynamics
ATDB	Aero Thermodynamic Data Base
CFD	Computational Fluid Dynamics
C/SiC	Carbon / Silicon Carbide
FLPP	Future Launchers Preparatory Program
IXV	Intermediate eXperimental Vehicle
SWBLI	Shock Wave Boundary Layer Interaction
TPS	Thermal Protection System
WTT	Wind Tunnel Tests

REFERENCES

1. J.P. Tribot, O. Lambert, O. Cantinaud, Ph. Tran, M. Prampolini, J.C Paulat, S. Guédron, *Pre-X Program : Aerothermodynamic objectives and aeroshape definition for in flight experiment,* IAC-02- V.5.03- October 2002.

2. E. Cosson, F. Thivet et Al., « Pre-X aerothermodynamics implications at system level », Atmospheric re-entry Symposium, March 21-23, 2005.